

ORIGINAL ARTICLE

High-Resolution Novel Indirect Bioprinting of Low-Viscosity Cell-Laden Hydrogels via Model-Support Bioink Interaction

Edgar Y.S. Tan,¹ Ratima Suntornnond,¹ and Wai Yee Yeong^{1,2}

Abstract

Bioprinting of unmodified soft extracellular matrix into complex 3D structures has remained challenging to fabricate. Herein, we established a novel process for the printing of low-viscosity hydrogel by using a unique support technique to retain the structural integrity of the support structure. We demonstrated that this process of printing could be used for different types of hydrogel, ranging from fast crosslinking gelatin methacrylate to slow crosslinking collagen type I. In addition, we evaluated the biocompatibility of the process by observing the effects of the cytotoxicity of L929 and the functionality of the human umbilical vein endothelium primary cells after printing. The results show that the bioprinted construct provided excellent biocompatibility as well as supported cell growth and differentiation. Thus, this is a novel technique that can be potentially used to enhance the resolution of the extrusion-based bioprinter.

Keywords: bioprinting, 3D printing, hydrogels, printing resolution, pluronic, alginate

Introduction

THE ABILITY TO design and print cell-embedded hydrogels that are high resolution is critical in biomedical research and organotypic tissue formation.^{1,2} Cytocompatibility, the resolution of cell placement and structural complexity, and the maturation of biologically active tissues are some of the challenges that bioprinting needs to address before it can be utilized as a tool for tissue culture.³ Bioprinted products such as skin-mimicking lamellar constructs comprising layers of keratinocytes and fibroblasts of <250 μm thickness have been generated through the use of laser-assisted bioprinting.⁴ While numerous other direct methods and strategies exist to print viable cell into a structure, such as the use of ink-jet, extrusion, and laser-induced forward transfer, the ability to print structures of good print resolution while obtaining good cell viability is somewhat limited. The printing resolution of hydrogel could often affect the long-term viability and metabolism of the cells embedded in the hydrogel.⁵ In one study, the effect of the spacing of the grooves affects the mass transport of media into a stiff hydrogel. This, in turn, greatly influenced the cellular metabolic and phenotypic activity of

the cells. In some cases, necrotic cores can be observed in embedded hydrogels that are caused by transport limitation.⁶

One of the conventional bioprinting techniques is the use of an extrusion-based printing technique. This form of printing dispenses a liquid using either a pneumatic or mechanical pump to create a positive pressure in the syringe. Extruding the solution in a controlled manner, this form of printing has been well documented in many studies as the process is simple and the machine is inexpensive.⁷ While the use of this process has been successful in fabricating 3D scaffolds and cell-embedded hydrogels, the live cell has to undergo tremendous shearing during dispensing as the material used has to be relatively viscous.^{8,9} As such, this process of printing would result in either lower cell viability or lower print resolution depending on the viscosity of the material used. One method of overcoming this challenge is the use of dual/multiple extrusion printing, in which two or more heads are used to dispense either scaffold hydrogel or cell-embedded hydrogel onto the platform.¹⁰ The use of multiple print heads is mainly common in the field of bioprinting as the gel stiffness is relatively weak and would require additional support to enable the structure to be stable.

¹Singapore Centre for 3D Printing (SC3DP), School of Mechanical and Aerospace Engineering, Nanyang Technological University, Singapore, Singapore.

²HP-NTU Digital Manufacturing Corporate Lab, School of Mechanical and Aerospace Engineering, Nanyang Technological University, Singapore, Singapore.

One of the supporting materials that has been used commonly is pluronic.^{11,12} Pluronic is a synthetic reverse thermoresponsive hydrogel. It has been widely used as a support material because it can be easily removed when the scaffold is immersed into cold liquid. Since pluronic is a physically crosslinked hydrogel, it is susceptible to absorb water from the surrounding, and when the concentration of pluronic in the hydrogel is below the critical gelation concentration, the hydrogel's structure would be eroded.¹³ As such, the interaction time between the pluronic and hydrogel of interest is usually instantaneous to prevent the gels from interacting. However, this is not possible for some natural occurring hydrogel that would need to be slowly cured over a period of time, such as collagen^{14,15} and Matrigel.¹⁶

Herein, we have developed a novel approach to indirectly print cell-embedded hydrogels using valve-based and dual-extrusion printing. In this method, the interaction between both the hydrogel of interest and pluronic is immobilized through the formation of an interfacial wall during printing. This interfacial wall would obstruct the solvent transport across the hydrogel, thereby forming a barrier to reduce diffusion of solutes across the interface during the curing process. Because of the interfacial wall, this technique can be applied to the low-viscosity hydrogel such as denaturalized gelatin methacrylate (GelMA) and collagen. Moreover, this interfacial barrier leads to better printing as well as provides good cell viability.

Materials and Methods

Fabrication of GelMA

GelMA was fabricated by the reaction between methacrylate anhydride and gelatin at 50°C in phosphate-buffered saline (PBS; Sigma-Aldrich) similar to the method that was previously described by Kazemzadeh-Narbat *et al.*¹⁷ The reaction was run for 2–3 h under a constant stirring condition in the dark. After which the reaction was terminated by diluting the solution fivefold with PBS. The diluted solution was further dialyzed with deionized water by using 12–14 kDa molecular-weight cutoff dialysis tubes (Sigma-Aldrich) for 1 week to remove excess methacrylate anhydride. Next,

the GelMA was frozen overnight at –90°C, lyophilized for 5–7 days until thoroughly dried, and stored at –30°C before further use.

Fabrication of support material and scaffold hydrogel

Support structure hydrogel was composed of 24.5% pluronic F127 (Sigma-Aldrich) and 2% alginate (Sigma-Aldrich) dissolved in deionized water. GelMA hydrogel was composed of 5% freeze-dried GelMA and 0.1 M of calcium chloride (CaCl₂) dissolved in deionized water, and pH of the solution is subsequently tuned to neutral (pH ≈ 7.0–8.0) by using 1 M NaOH, which was added in a dropwise manner. Collagen hydrogel was composed of 2 mg/mL of high-concentration type I collagen (354249; Corning), and 0.1 M CaCl₂ was subsequently added to the solution.

Evaluation of surface interaction of calcium ions on pluronic structure

A square structure of lengths 1 × 1 cm², height (thickness) of 2 mm, and a z layer resolution of 0.2 mm was designed in BioCAD™, which is the software that integrated with BioFactory bioprinting (Regenhu, Villaz-St-Pierre, Switzerland). The structure was printed by using a pneumatic extrusion-based bioprinter. Subsequently, 100 μL of the GelMA solution with CaCl₂ was added to simulate the interaction between the Ca²⁺ cation and the alginate in the pluronic structure. To ensure that the thickness of the material is consistent and the test to be unbiased, a fixed concentration of alginate and pluronic was used while varying the calcium concentration.

Printability test and printing of 3D complex structure

A grid CAD file was designed using BioCAD, which attached to the pneumatic extrusion-based bioprinter. The model hydrogel and the support hydrogel were loaded in 5 mL syringe before printing. The printing condition of all concentrations was at stage moving speed of 500 mm/min, pressure of 5 bar, and temperature at 27°C ± 2°C (room temperature). Twenty-seven-gauge (210 μm inner diameter) nozzle was used for printing. As shown in Figure 1, after

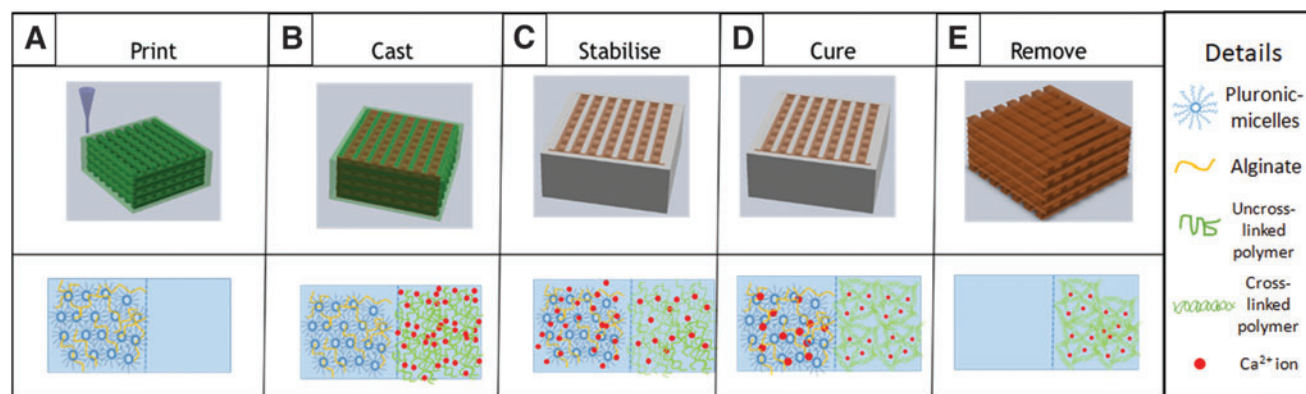


FIG. 1. Schematic of the fabrication process for 3D hydrogel scaffolds. (A) Printing of sacrificial alginate/pluronic mold. (B) Dispensing of collagen/GelMA solution into the mold structure. (C) Interfacial reaction between the sacrificial hydrogel and collagen/GelMA solution. (D) Curing of hydrogel either via UV crosslinking for GelMA or thermal incubation for collagen. (E) Removal of support by soaking the printed structure in cold PBS solution. GelMA, gelatin methacrylate; PBS, phosphate-buffered saline. Color images are available online.

printing, the GelMA hydrogel samples were cured by using the UV flood curing system (Techno Digm, Singapore) for 120 s and soaked in cold PBS for 15 min before further experimentation. For the collagen structure, the samples were cured in an incubator at 37°C for 30 min before being soaked in cold PBS to remove the pluronic/alginate support structure.

Cell viability and cell proliferation test

L929 mouse fibroblast cells were embedded in the hydrogel with a cell density of 2×10^6 cells/mL before printing. A total of 12 bioprinted samples were plated on a 24-well plate. Cells were cultivated in high-glucose Dulbecco's modified Eagle's medium (Sigma-Aldrich) supplemented with 10% (v/v) fetal bovine serum (PAA Laboratories, Inc.; GE Healthcare) and 1% (v/v) antibiotic/antimycotic solution (PAA; GE Healthcare). Culture medium was replaced every 2–3 days and cells were grown at 37°C in the presence of 5% CO₂. The experiment was sampled at days 1, 3, and 7 for live/dead staining and PrestoBlue® test. For live/dead staining, the cell culture medium was removed from the sample, followed by washing the samples with PBS for two to three times. The Live/Dead Cell Double Staining Kit (Sigma-Aldrich, USA) was used to validate cell compatibility of the hydrogels. Solution A (calcein AM solution) and solution B (propidium iodide solution) were added into each sample at the ratio of 2:1 in PBS solution to form the assay solution. One hundred microliters of assay solution were added into each well, and the well was incubated at 37°C for 15 min. Then, cell viability was detected under fluorescence light using a fluorescence microscope with 490 nm excitation for live cells, and at 545 nm excitation, only dead cells can be observed. For the PrestoBlue test, the cell culture experiment was stopped by adding PrestoBlue solution (Invitrogen; Life Technologies, USA) into cell culture medium using a ratio of 1:9 by volume and the well was incubated at 37°C for 2 h. Then, the cell number was detected by using a microplate reader (SPARK 10M; Tecan) with 560 nm excitation and at 590 nm emission.

Scanning electron microscope analysis

Before scanning electron microscope (SEM) analysis, the samples were required to undergo two steps of fixation. For primary fixation, 2.5% v/v glutaraldehyde solution (Sigma-Aldrich, USA) was used. All samples were soaked in 2.5% v/v glutaraldehyde solution for 1 h at 25°C. After that, samples were washed with distilled water several times to remove excess glutaraldehyde. Next, ethanol was used to dehydrate the cells by a series of concentrations (v/v): 25%, 50%, 70%, 95%, 100%, and 100%. Samples were soaked in each ethanol concentration for 10 min. After which, samples were washed with distilled water and dried in a desiccator for 1 day. Next, the hydrogel samples were coated with gold at 10 mA for 20 s before the SEM inspection.

DAPI/F-actin staining

Human umbilical vein endothelium primary cells (HUVEC; Lonza) with a passage number of 5–6 were cultivated in the Endothelial Growth BulletKit (EGM-2; Lonza) supplemented with 1% antibiotic/antimycotic solution (PAA; GE Healthcare). Culture medium was replaced every 2–3 days

and cells were grown at 37°C in the presence of 5% CO₂. After the cells reached more than 80% confluence, they were subcultured by using Trypsin/EDTA (CC-5012; Lonza) and mixed with the 2 mg/mL collagen at a cell density of 3×10^6 cells/mL. The bioprinted samples were plated on a 24-well plate and soaked in a cell culture medium for 30 min to remove the sacrificial materials. After that, they were stained by ActinGreen™ 488 ReadyProbes® (Life Technologies; Thermo Fisher) and NucBlue® Live ReadyProbes (Life Technologies; Thermo Fisher) reagents and observed under an inverted microscope (Axio Vert.A1; Carl Zeiss).

Immunofluorescence

HUVECs were cultivated as described above. For immunofluorescence, the cell-laden hydrogel samples were plated into 24-well plates up until day 7. To investigate the cell differentiation of HUVECs, CD31 and von Willebrand factor (vWF) expression was selected. The samples were rinsed in Dulbecco's phosphate-buffered saline (DPBS) a few times and fixed in 4% formaldehyde solution (Sigma-Aldrich, USA) in DPBS (HyClone; GE Life Sciences) for 30 min. After that, the samples were soaked in blocking solution (5 wt % BSA, 0.5 wt % Tween 20 in DPBS) for 2 h at room temperature. Subsequently, the cell membranes were permeabilized in 0.25% (v/v) Triton X-100 (Bio-Rad, USA) in blocking solution for 20 min and washed with DPBS three times. The samples were soaked in the primary antibody staining with 1/100 dilution of mouse monoclonal anti-CD31 antibody (Life Technologies; Thermo Fisher) and 3 µg/mL of vWF mouse monoclonal antibody (Life Technologies; Thermo Fisher) in DPBS overnight at 4°C. The samples were washed with blocking solution three times with 5-min intervals between the washing steps. After primary antibody staining, the samples were added with 1/500 dilution of Alexa Fluor-555-conjugated goat anti-mouse secondary antibodies (Life Technologies; Thermo Fisher) in DPBS for 2.5 h at ambient condition. Subsequently, the samples were washed in blocking solution three times with 15-min intervals between the washing steps, followed by a drop of NucBlue (Life Technologies; Thermo Fisher) staining for 20 min. After rinsing, fluorescent images were taken by using a fluorescent microscope (Axio Vert.A1; Carl Zeiss).

Hematoxylin and eosin staining

The samples were fixed with formaldehyde (10% v/v) overnight followed by dehydration with ethanol in a series of concentrations (v/v): 70%, 80%, 95% (twice), and 100% (three times). Samples were soaked in each ethanol concentration for 45 min. Later, samples were immersed in xylene for three times with a 45-min interval each time. Subsequently, the samples were embedded in paraffin, and 7 µm sections were cut by using a microtome (Leica, Germany). The sections were immersed in a water bath at 37°C and mounted on Polysine® adhesive-coated glass slides for better adhesion. The slides were left to dry overnight at 37°C. The sections were rehydrated in xylene and then a decreasing series of alcohol concentrations, 100%, 95%, and 70%, followed by immersing in water. Conventional hematoxylin and eosin (H&E; Sigma, USA) staining was performed, and the samples were dried for a few hours. Slides were examined under light microscopy.

Statistical analysis

The statistical significance was determined by a Student's *t*-test study for two groups of data or analysis of variance. *p*-Values were presented as statistically significant and highly significant at 95% level of confidence as **p* < 0.05, ***p* < 0.05 is for significantly different from the rest.

Results and Discussion

Evaluation of surface interaction of calcium ions in an alginate/pluronic support structure

The stability of the support material after interaction with calcium was evaluated to confirm and optimize the competency of using alginate/pluronic as a support structure. As shown in Figure 2, there was minimal change in the dimension to the dimension when the calcium concentration is between 50 and 100 mM for more than 2.5 min. The calcium ions resulted in slight swelling due to the formation of calcium/alginate interaction in the pluronic hydrogel.¹⁸ If an excessive amount of calcium ions were used, the structure would expand uncontrollably. This is possibly due to the calcium ions displacing the stable micelle structure and reducing the interaction between the pluronic chains, thus causing a destabilization of the pluronic structure. If pure

pluronic was used in the reaction, the solvent (water) would interact and lower the concentration of pluronic on the surface of the hydrogel/solvent interface, resulting in an erosion of the pluronic structure. From this result, it can be concluded that the use of an alginate/pluronic structure with an optimized calcium concentration would result in a structurally stable support structure that could withstand solvent interaction.

Solvation of pluronic support structure

Electrostatic interaction plays a vital role in the structural properties of hydrogels. Slight changes in the pH, solute concentrations, and their temperature could result in changes in their physical properties. This is due to the interaction of the polar and ionic molecules interacting with the polar solvent (water). The hydrogel's range of deformation is dependent on the presence of the interacting groups and their distribution on the molecule.

The interaction between pluronic and water is illustrated in Figure 3B. Initially, pluronic gel acts as its own a membrane against the solvent. Hydrostatic pressure will exist between the interior of the gel and the water phase. Thus, a pressure gradient exists through the interface. This presence of hydrostatic pressure is influenced by the swelling pressure that

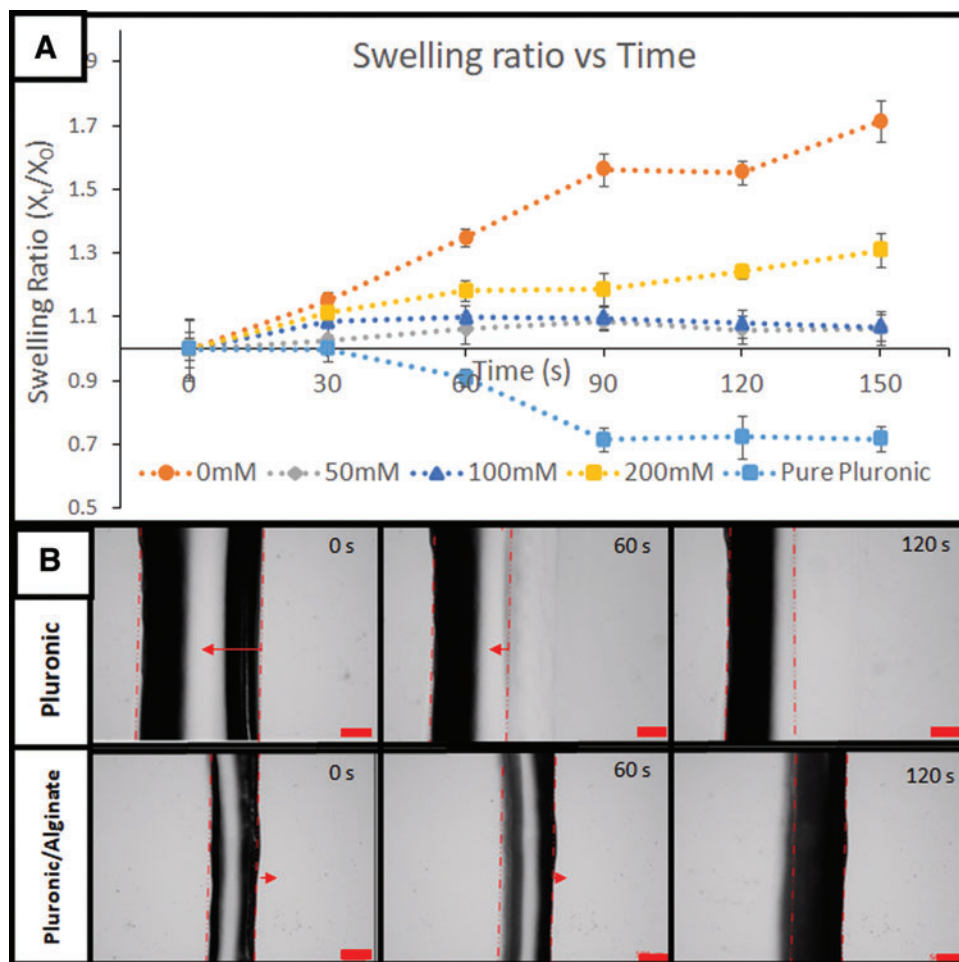


FIG. 2. (A) Comparison of the effects of the type and concentration of support structure changes over time and (B) microscopy evidence on the effect of using pluronic as support compared with pluronic/alginate, using calcium-GelMA printing material. Scale bar: 500 μ m. Color images are available online.

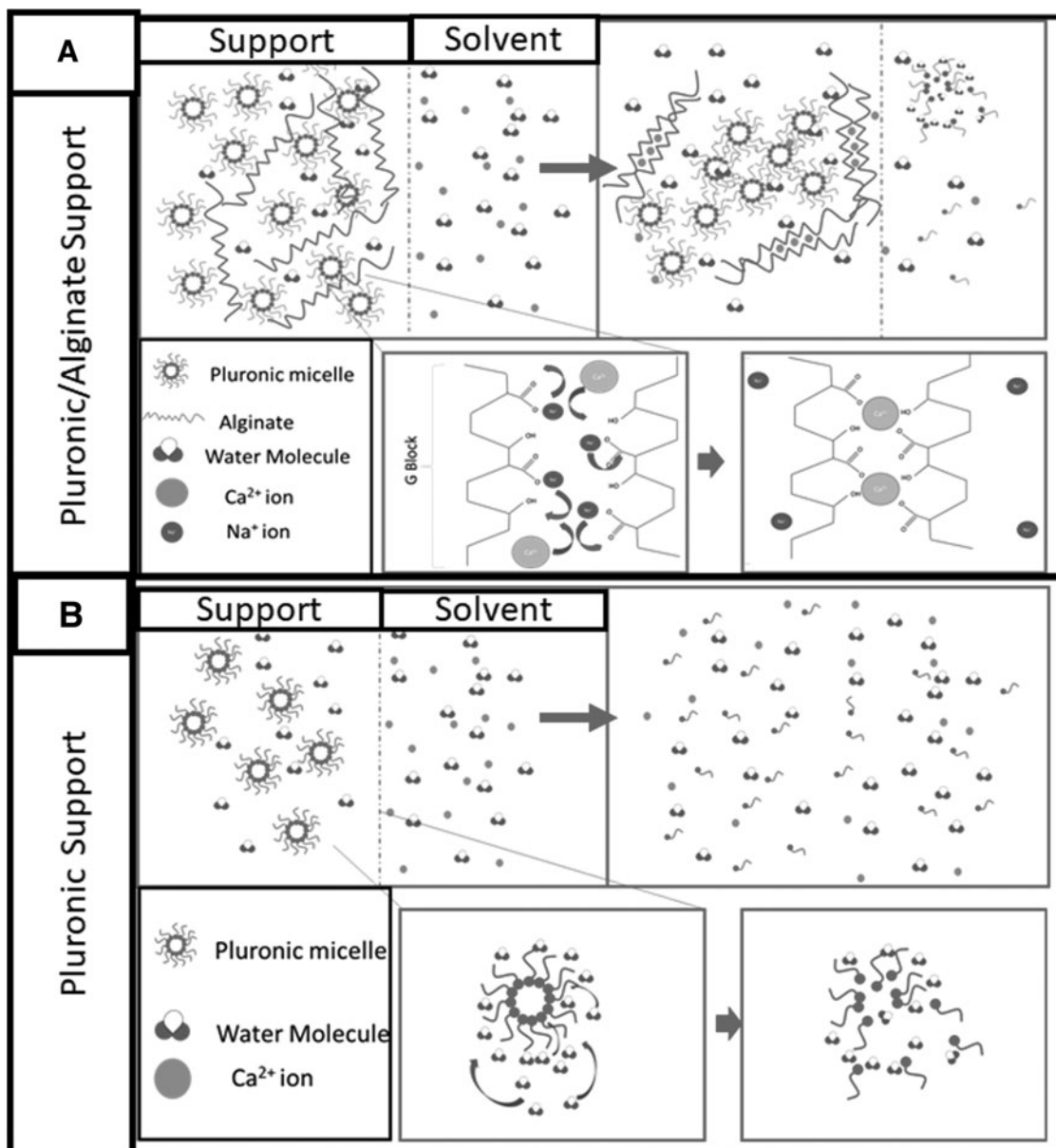


FIG. 3. Comparison of interaction interface of solvent on (A) pluronic/alginate support and (B) pluronic hydrogel in divalent calcium ion water.

is exerting on the gel to prevent it from swelling. This rise in hydrostatic pressure increases the chemical potential of the water in the hydrogel to match that of the solvent outside the membrane. However, for pure pluronic, this rise of the solvent concentration in the hydrogel causes a nonvolume preserving deformation on the gel. Due to the weaker H-bond interaction between pluronic molecules, the increase in water molecules competes and displaces the pluronic molecules. This disrupts the micelle structure and reduces the pluronic hydrogel back to its solution state. This interaction will happen until the solvent has almost similar pluronic concentration as the pluronic critical micelle concentration.

The addition of alginate, as illustrated in Figure 3A, provides a better approach to produce a support structure. In this system, calcium ions are adsorbed onto the surface of the alginate/pluronic hydrogel. The calcium displaces the so-

dium ions on the alginate chains, thereby forming an ionic crosslink within the hydrogel. Over time, as more of the alginate interacted, the gel interaction would be increasingly stabilized and produces a robust membrane in the hydrogel. The formation of calcium/alginate helps to facilitate a reduction in the pluronic/solvent interaction by forming a stronger ionic interaction with the neighboring alginate and reducing the erosion of pluronic into the solvent. This is significant as this would reduce the pluronic-based hydrogel material.

In vitro evaluation of hydrogel process

L929 fibroblast cells have been frequently used for the preliminary biocompatibility test.¹⁹ To enable the optimal survivability of cells embedded in the hydrogel, the pH of the

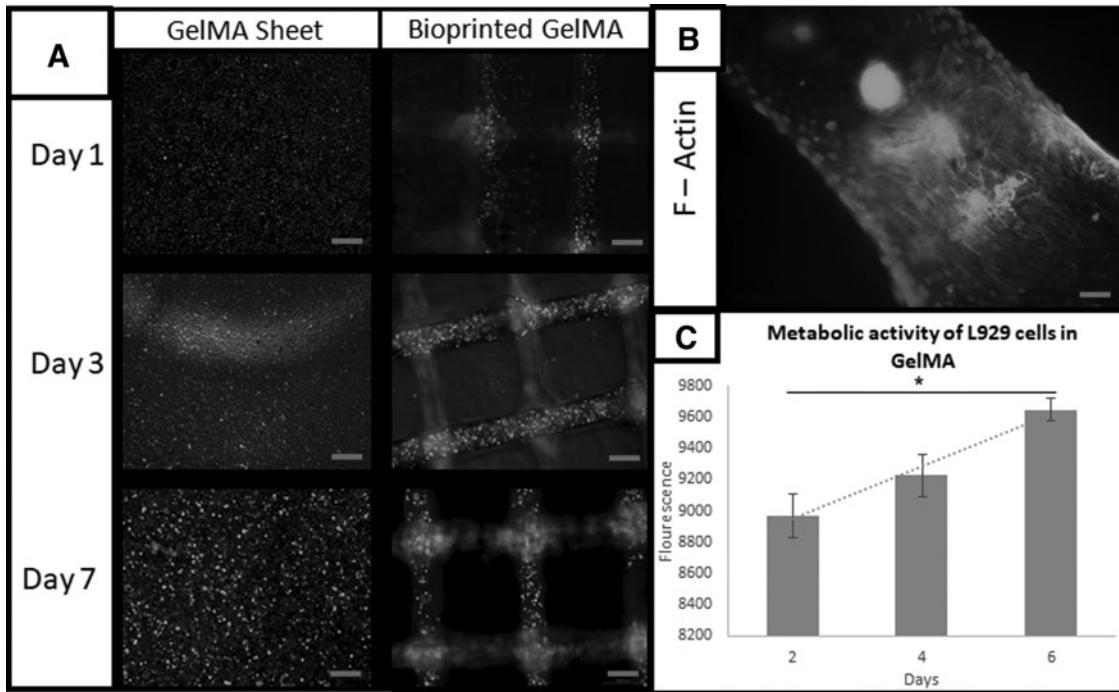


FIG. 4. (A) Comparison of Live/Dead Assay on L929 over 7 days (magnification: $\times 5$). (B) F-actin staining of L929 after 14 days (magnification: $\times 40$) and (C) metabolic activity of L929s in GelMA from day 2 to 6 ($n=3$), scale of (A): $200\ \mu\text{m}$ and scale of (B): $20\ \mu\text{m}$.

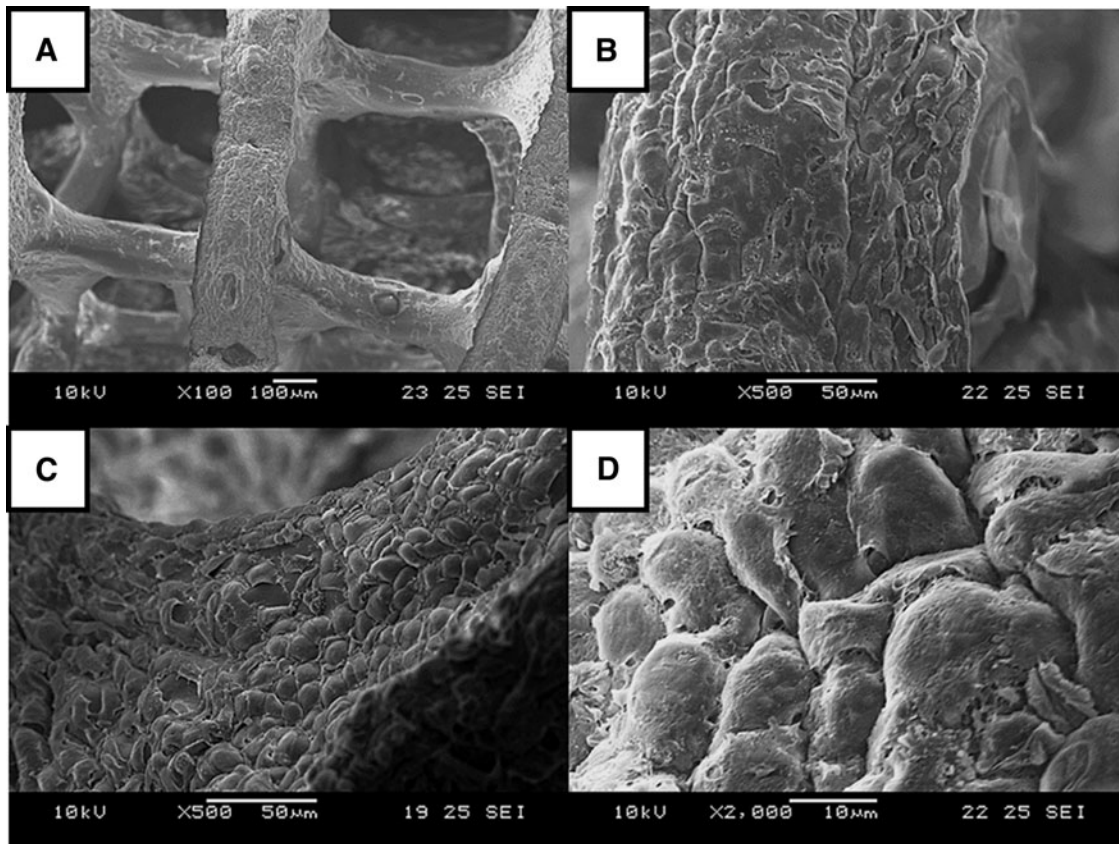


FIG. 5. SEM images of L929 (day 14) on GelMA, at different magnifications: (A) $\times 100$, (B) $\times 500$, (C) $\times 500$, and (D) $\times 2000$. SEM, scanning electron microscope.

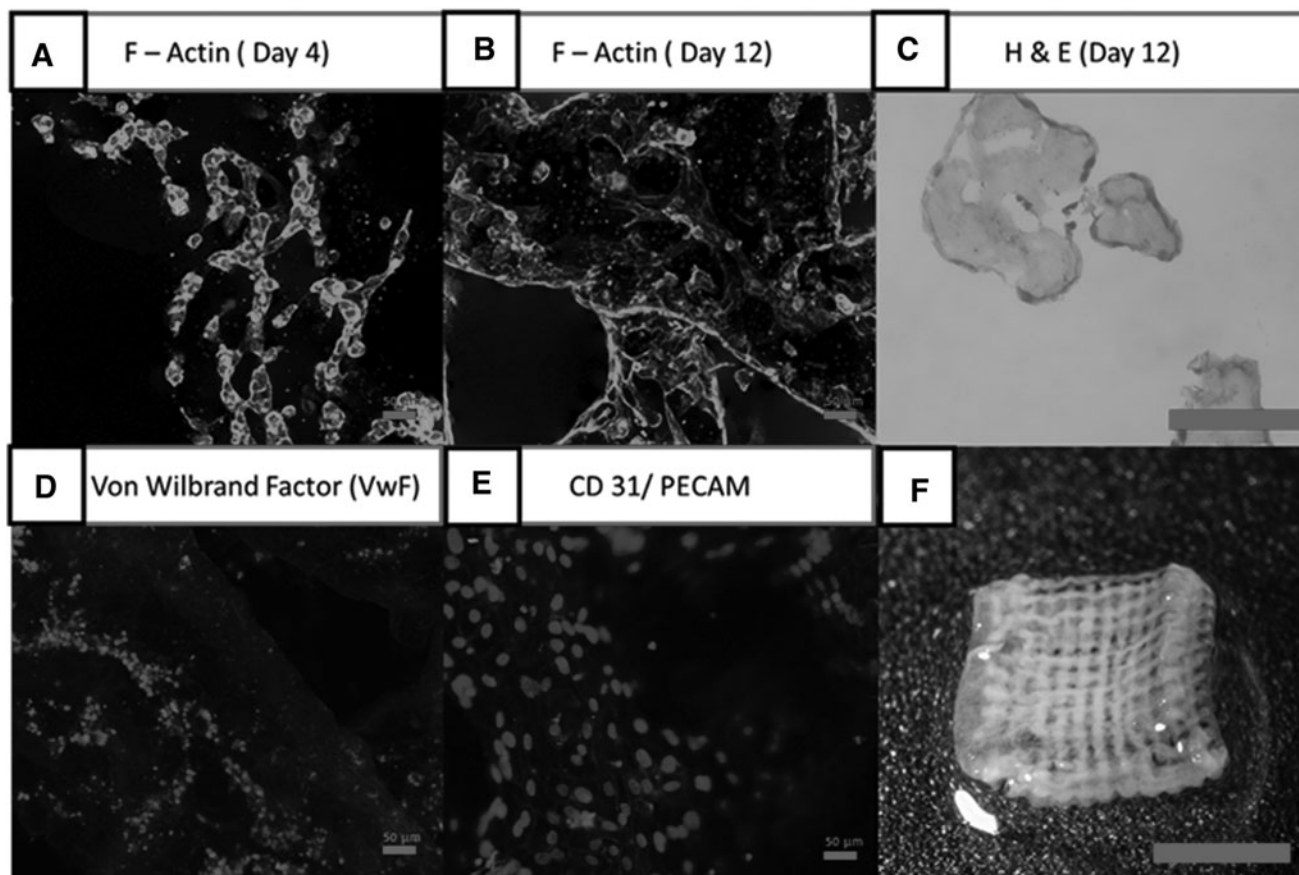


FIG. 6. (A) F-actin on day 4 indicating initial phase of differentiation, scale: $\times 20$. (B) F-actin on day 12 indicating mature stage of differentiation, scale: $\times 20$ (scale bar: $50 \mu\text{m}$). (C) Hematoxylin and eosin (day 12) staining to indicate size and cell distribution within the hydrogel, scale: $\times 20$. (D) Von Willebrand factor to determine platelet adhesion functionality, scale: $\times 20$. (E) CD31 to determine cell adhesion functionality of HUVECs, scale: $\times 20$. (F) Collagen scaffold seeded with HUVECs after day 12, scale: 5 mm. HUVEC, human umbilical vein endothelium primary cell.

printing solution was tuned to ~ 7 and the osmolarity of the solution to be between 200 and 300 mmol, which is the physiological comparison. In this experiment, L929 was mixed with 5% Ca-GelMA solution. As shown in the live/dead results in Figure 4A and the PrestoBlue result in Figure 4C, it can be concluded that the alginate/pluronic support structure does not have any effect on affecting the cell viability of the cells in the hydrogel. The increasing trend from the cell viability assay demonstrated that the cells are proliferating at an accumulative rate, similar to the results from the tissue culture plate culture. The initial cell death could have resulted from the use of a photoinitiator in the hydrogel.²⁰ The actin staining in Figure 4B and SEM images in Figure 5 show that the cells have migrated to the surface, which they adhered and spread throughout the scaffold. This provides evidence that the pluronic in this system has low to none effect on cell adhesion and cell proliferation.

To evaluate if this process can be used for angiogenesis study, HUVECs were used to evaluate this property in the experiment. As HUVECs are much more sensitive to the environment compared with L929 cells, the base solution was altered to a collagen-based solution instead. In addition, the use of a collagen-based solution further helps evaluate the stability of the structure over long periods (30 min). The

use of HUVECs would help to determine if the support material would affect cell differentiation and other cellular functions. On the 10th day, as shown in Figure 6D and E, HUVECs were alive and expressing cell markers CD31 and vWF. This indicates that the HUVECs still have the function of endothelial cells.²¹⁻²³ The HUVECs did indicate signs of fusion as their metabolic activity was lowered continuously since the second day, as shown in Figure 7. Another possible

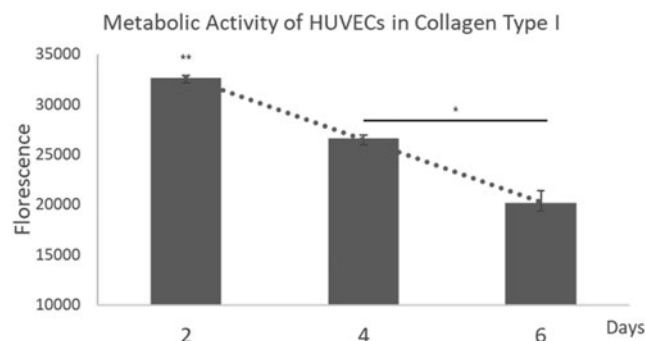


FIG. 7. Metabolic activity of HUVECs in collagen from day 2 to 6 ($n=3$).

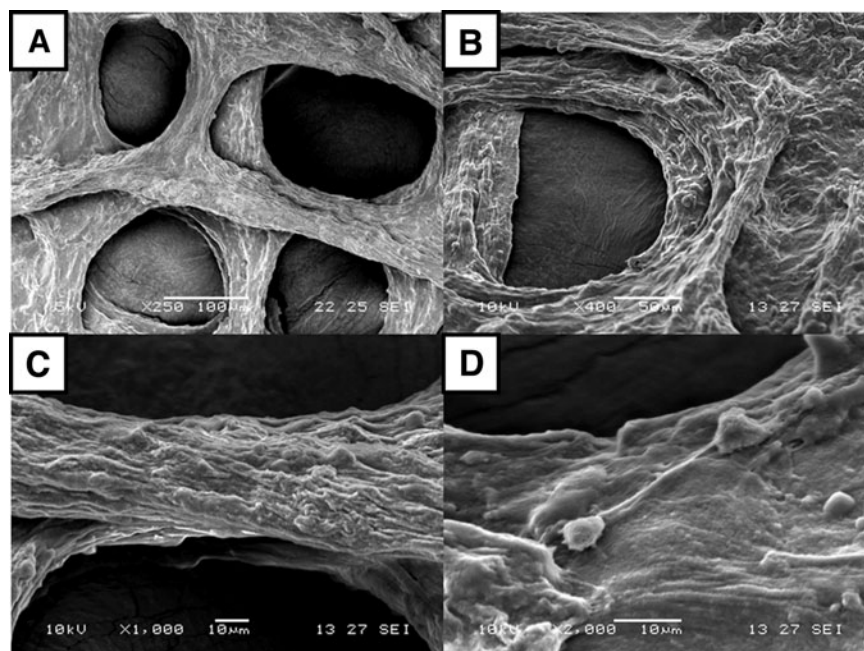


FIG. 8. SEM image of HUVECs embedded in collagen type I at different magnifications: (A) $\times 250$, (B) $\times 400$, (C) $\times 1000$, and (D) $\times 2000$.

reason is due to the shrinkage of the collagen sample, thus causing the fluorescence signal to overlap. However, as shown in Figure 6B, a 12-day study showed that the cells are uniformly distributed on the surface of the collagen scaffold with no evidence of clumping. This can also be seen from the H&E staining (Fig. 6C). Signs of collagen remodeling can be observed as after 12 days the collagen hydrogel shrunk and turned opaque²⁴ (Fig. 6F).

Evaluation on resolution and accuracy of printed construct

The resolution and accuracy of the printed construct demonstrate the effectiveness of this process of bioprinting.²⁵ For both the GelMA and collagen constructs, the overall features of the hydrogels are still similar to the initially printed products even after 7 days of culture. Due to the difference in stiffness and concentration difference between GelMA and collagen, shrinkage in collagen can be expected to be higher. In both materials, a resolution of $\sim 100 \mu\text{m}$ can be obtained,

as shown in Figures 5 and 8, but it might not be representative throughout the entire structure. Depending on the depth, the density of the hydrogel, and the interaction between the support materials, the resolution of the struts would vary. To mitigate these differences in print accuracy, the base hydrogel could be printed on every layer to reduce the differences caused by this form in indirect printing.

Moreover, from FRESH V2.0 3D printing work, as given in Lee *et al.*,²⁶ our technique is similar to them, both methods use the principle of the model and support material interaction, but our method can perform on the solid platform directly. Thus, this technique will save time on the preparation of the material, especially on the slurry part, and by using a jetting bioprinting technique, the samples can be fabricated within a few minutes. Nonetheless, the advantage of FRESH V2.0 technique is that it can print curvature feature easily. By using high concentration similar to FRESH V2.0 work, we might be able to obtain higher resolution due to the shrinkage of collagen. Another advantage is that we can use multi-materials with different printheads. This is because alginate

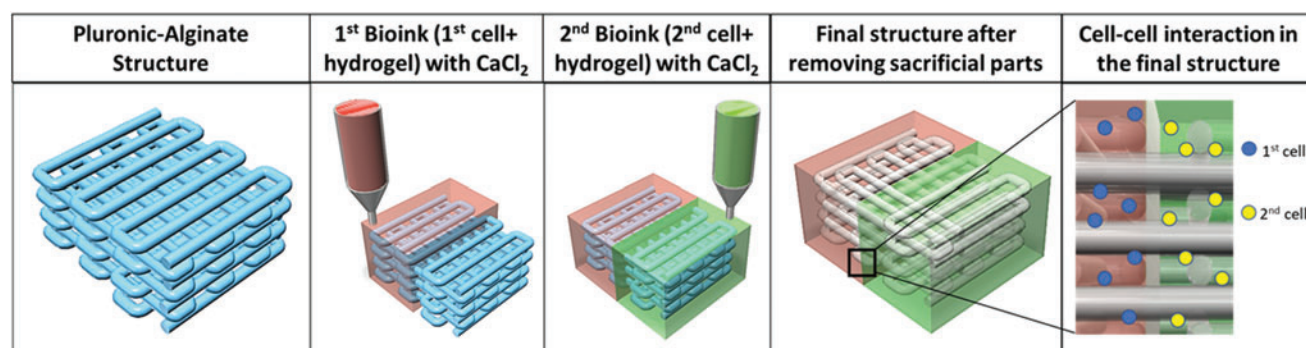


FIG. 9. Multimaterial hollow structure fabricated by the interaction between pluronic/alginate and bioink- CaCl_2 . CaCl_2 , calcium chloride. Color images are available online.

and CaCl₂ were used as blocking barrier. Thus, one side can be one material, and another side can be another bioink, as shown in Figure 9. This technique opens another potential of high-resolution scaffold with a vascularized hollow feature.

Conclusion

In this research, an indirect method of bioprinting has been successfully developed. By using an alginate/pluronic support structure, low-viscosity cell-laden hydrogels can be fabricated. The interaction between Ca²⁺ and alginate helps to prevent osmosis interaction between the two hydrogels (model and support structure). The long-term stability of the support material helps to enable sufficient mechanical strength for any form of low-viscosity hydrogel, including GelMA and collagen hydrogels. From the *in vitro* evaluation, both L929 and HUVECs survived over 7 days in all the samples. The cells were able to migrate, proliferate, and show the sign of functionality. Both cells can attach and pack together. The presence of actin showed that the cells are fusing, while the presence of CD31 and vWF showed the endothelium cells' functionality as well as the efficiency of vascularization. This provided that indirect bioprinting and support material support cell growth and cell differentiation. This process of printing helps to enable the printing of more desirable hydrogel without the need to be concerned about the printability of the cell-laden hydrogels. Therefore, this work offers an excellent potential for future bioprinting hydrogels and does not limit the type of hydrogels for tissue engineering and biomedical applications. With the advent of the use of microvalve technology, the resolution of the printed structure could be further enhanced to cater for smaller features if required.

Authors' Contributions

E.Y.S.T. performed all of the experiments. R.S. was involved and performed HUVEC-related experiments. This article was written through the contributions of all authors. All authors have given approval to the final version of the article.

Author Disclosure Statement

No competing financial interests exist.

Funding Information

This work would not have been possible without the financial support of the Nanyang Technological University-National Healthcare Group Ageing Research Grant (NTU-NHG ARG; Grant number: ARG-14009). This work is also part of Mr. Edgar Yong Sheng Tan's thesis, more information about which can be found from Ref.²⁷

References

- Kengla C, Renteria E, Wivell C, *et al.* Clinically relevant bioprinting workflow and imaging process for tissue construct design and validation. *3D Print Addit Manuf* 2017; 4:239.
- An J, Teoh JEM, Suntornond R, *et al.* Design and 3D printing of scaffolds and tissues. *Engineering* 2015;1:261.
- Graham AD, Olof SN, Burke MJ, *et al.* High-resolution patterned cellular constructs by droplet-based 3D printing. *Sci Rep* 2017;7:7004.
- Michael S, Sorg H, Peck C-T, *et al.* Tissue engineered skin substitutes created by laser-assisted bioprinting form skin-like structures in the dorsal skin fold chamber in mice. *PLoS ONE* 2013;8:e57741.
- Lee MK, Rich MH, Baek K, *et al.* Bioinspired tuning of hydrogel permeability-rigidity dependency for 3D cell culture. *Sci Rep* 2015;5:8948.
- Tsang VL, Chen AA, Cho LM, *et al.* Fabrication of 3D hepatic tissues by additive photopatterning of cellular hydrogels. *FASEB J* 2007;21:790.
- Bandyopadhyay A, Dewangan VK, Vajanthri KY, *et al.* Easy and affordable method for rapid prototyping of tissue models in vitro using three-dimensional bioprinting. *BioCybernet Biomed Eng* 2018;38:158.
- You F, Eames BF, Chen X. Application of extrusion-based hydrogel bioprinting for cartilage tissue engineering. *Int J Mol Sci* 2017;18:1597.
- Markstedt K, Sundberg J, Gatenholm P. 3D bioprinting of cellulose structures from an ionic liquid. *3D Print Addit Manuf* 2014;1:115.
- Kang H-W, Lee SJ, Ko IK, *et al.* A 3D bioprinting system to produce human-scale tissue constructs with structural integrity. *Nat Biotechnol* 2016;34:312.
- Naomi P, Willi S, Thomas B, *et al.* Proposal to assess printability of bioinks for extrusion-based bioprinting and evaluation of rheological properties governing bioprintability. *Biofabrication* 2017;9:044107.
- Suntornond R, Tan EYS, An J, *et al.* A highly printable and biocompatible hydrogel composite for direct printing of soft and perfusable vasculature-like structures. *Sci Rep* 2017;7:16902.
- Suntornond R, An J, Chua CK. Bioprinting of thermo-responsive hydrogels for next generation tissue engineering: a review. *Macromol Mater Eng* 2017;302:1600266.
- Liu GY, Agarwal R, Ko KR, *et al.* Templated assembly of collagen fibers directs cell growth in 2D and 3D. *Sci Rep* 2017;7:9628.
- Wei Long N, Jovina Tan Zhi Q, Wai Yee Y, *et al.* Proof-of-concept: 3D bioprinting of pigmented human skin constructs. *Biofabrication* 2018;10:025005.
- Jang JM, Tran S-H-T, Na SC, *et al.* Engineering controllable architecture in matrigel for 3D cell alignment. *ACS Appl Mater Interf* 2015;7:2183.
- Kazemzadeh-Narbat M, Rouwkema J, Annabi N, *et al.* Engineering photocrosslinkable bicomponent hydrogel constructs for creating 3D vascularized bone. *Adv Healthcare Mater* 2017;6:1601122.
- Qin Y. The gel swelling properties of alginate fibers and their applications in wound management. *Polym Adv Technol* 2007;19:6.
- Serrano MC, Pagani R, Vallet-Regí, M., *et al.* In vitro biocompatibility assessment of poly(ϵ -caprolactone) films using L929 mouse fibroblasts. *Biomaterials* 2004;25:5603.
- Williams CG, Malik AN, Kim TK, *et al.* Variable cyto-compatibility of six cell lines with photoinitiators used for polymerizing hydrogels and cell encapsulation. *Biomaterials* 2005;26:1211.
- Turner NA, Nolasco L, Ruggeri ZM, *et al.* Endothelial cell ADAMTS-13 and VWF: Production, release, and VWF string cleavage. *Blood* 2009;114:5102.

22. Müller AM, Hermanns MI, Skrzynski C, *et al.* Expression of the endothelial markers PECAM-1, vWf, and CD34 in vivo and in vitro. *Exp Mol Pathol* 2002;72:221.
23. Datta P, Ayan B, Ozbolat IT. Bioprinting for vascular and vascularized tissue biofabrication. *Acta Biomater* 2017;51:1.
24. McGuigan AP, Sefton MV. The thrombogenicity of human umbilical vein endothelial cell seeded collagen modules. *Biomaterials* 2008;29:2453.
25. Tan EYS, Yeong WY. Concentric bioprinting of alginate-based tubular constructs using multi-nozzle extrusion-based technique. *Int J Bioprint* 2015;1:49–56.
26. Lee A, Hudson A, Shiwarski D, *et al.* 3D bioprinting of collagen to rebuild components of the human heart. *Science* 2019;365:482.
27. Tan EYS. Biofabrication of choroid-retina tissue construct for modelling of age-related macular degeneration disease. 2019. PhD Thesis. <https://dr.ntu.edu.sg/handle/10356/105573> (last accessed November 20, 2020).

Address correspondence to:

Ratima Suntornnond
Singapore Centre for 3D Printing (SC3DP)
School of Mechanical and Aerospace Engineering
Nanyang Technological University
50 Nanyang Avenue
Block N3.1-B2C-03
Singapore 639798

E-mail: ratima001@e.ntu.edu.sg